

# Synthesis and characterisation of $\{\text{Mo}(\eta\text{-L})(\text{CO})_3\}^+$ ( $\eta\text{-L} = \text{C}_5\text{H}_5$ or $\text{C}_5\text{Me}_5$ ) fragments ligated with $[\text{CB}_{11}\text{H}_{12}]^-$ and derivatives. Isolation and structural characterisation of an intermediate in a silver salt metathesis reaction

Nathan J. Patmore,<sup>a</sup> Mary F. Mahon,<sup>a</sup> Jonathan W. Steed<sup>b</sup> and Andrew S. Weller<sup>a\*</sup>

<sup>a</sup> Department of Chemistry, University of Bath, Bath, UK BA2 7AY

<sup>b</sup> Department of Chemistry, Kings College London, The Strand, London, UK WC2R 2LS

Received 12th October 2000, Accepted 22nd November 2000

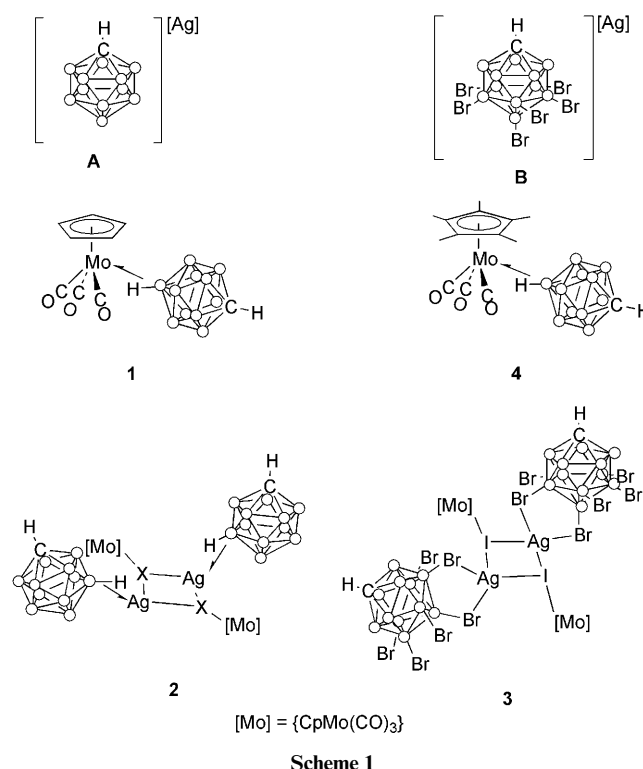
First published as an Advance Article on the web 11th January 2001

The synthesis of  $\{\text{Mo}(\eta\text{-L})(\text{CO})_3\}^+$  ( $\eta\text{-L} = \text{C}_5\text{H}_5$  or  $\text{C}_5\text{Me}_5$ ) fragments, ligated to the mono-anionic, weakly co-ordinating, carboranes  $[\text{closo-1-CB}_{11}\text{H}_{12}]^-$  and  $[\text{closo-CB}_{11}\text{Br}_6\text{H}_6]^-$ , has been investigated. Treatment of  $[\text{MoCp}(\text{CO})_3\text{X}]$  ( $\text{X} = \text{Cl}$  or  $\text{I}$ ) with  $\text{Ag}[\text{CB}_{11}\text{H}_{12}]$  eventually affords the zwitterionic complex  $[\text{MoCp}(\text{CO})_3(x\text{-}\mu\text{-H-1-CB}_{11}\text{H}_{12})]$  ( $x = 12$  or  $7$ ), via an intermediate dimeric species  $[\text{MoCp}(\text{CO})_3\text{X}\cdot\text{Ag}(\text{CB}_{11}\text{H}_{12})_2]$ . For  $\text{X} = \text{I}$  this intermediate has been characterised by  $^1\text{H}$ ,  $^{11}\text{B}$  NMR spectroscopy and X-ray crystallography and represents the first structurally characterised intermediate in a silver salt metathesis reaction. When the less nucleophilic carborane  $[\text{CB}_{11}\text{Br}_6\text{H}_6]^-$  (as its silver salt) is used metathesis is halted at the intermediate stage, affording the complex  $[\text{MoCp}(\text{CO})_3\text{I}\cdot\text{Ag}(\text{CB}_{11}\text{Br}_6\text{H}_6)]_2$ . Silver salt metathesis does not proceed using the sterically more demanding  $[\text{Mo}(\text{Cp}^*)(\text{CO})_3\text{I}]$ , with only intractable products isolated. The carborane anion can be introduced into the co-ordination sphere of this complex by reaction of  $[\text{H}(\text{OEt}_2)_x][\text{CB}_{11}\text{H}_{12}]$  with  $[\text{Mo}(\text{Cp}^*)(\text{CO})_3\text{Me}]$  affording  $[\text{Mo}(\text{Cp}^*)(\text{CO})_3(x\text{-}\mu\text{-H-1-CB}_{11}\text{H}_{12})]$  ( $x = 12$  or  $7$ ). All new compounds have been characterised by multinuclear NMR spectroscopy and X-ray crystallography.

## Introduction

The use of mono-anionic icosahedral carboranes as candidates for the 'least co-ordinating' anions has been championed by work from the groups of Reed<sup>1</sup> and Strauss.<sup>2</sup> Elegant demonstrations of the high chemical inertness and low nucleophilicity of these anions has recently been demonstrated by the isolation of protonated benzene as a weighable, room temperature stable, crystalline solid<sup>3</sup> and the use of perfluorinated  $[\text{1-Et-CB}_{11}\text{F}_{11}]^-$  to isolate normally inaccessible organometallic compounds.<sup>4</sup> However, to date, there have been few studies associated with the co-ordination chemistry of  $[\text{CB}_{11}\text{H}_{12}]^-$ , and its derivatives, with transition metal fragments. This is perhaps surprising as many academically and commercially relevant processes rely on the generation, and subsequent stabilisation, of Lewis acidic fragments. Studies of the chemistry of  $[\text{CB}_{11}\text{H}_{12}]^-$  associated with Group 4,<sup>5</sup> 8<sup>6</sup> and 10<sup>7</sup> cations have appeared, while related chemistry utilising mono- and di-anionic rhenacarboranes has recently been reported by Stone and co-workers with respect to reactivity with transition metal fragments.<sup>8</sup> Compared to the other major, now ubiquitous, least co-ordinating anion  $[\text{BAr}_f]^-$ ,<sup>9</sup> and derivatives thereof  $[\text{BAr}_f = \text{B}(\text{C}_6\text{F}_5)_4 \text{ or } \text{B}\{\text{C}_6\text{H}_3(\text{CF}_3)_2\}_4]$ , the transition metal chemistry associated with  $[\text{CB}_{11}\text{H}_{12}]^-$  is underdeveloped. With this in mind we are interested in using carborane anions as weakly co-ordinating anionic ligands, stabilising reactive Lewis-acidic metal fragments by offering a 'virtual co-ordination site'.<sup>10</sup>

In this investigation we have initially chosen  $[\text{Mo}(\eta\text{-L})(\text{CO})_3\text{X}]$  as one of the systems to study. The ability systematically to vary the ancillary  $\pi$  ligands (e.g.  $\eta\text{-L} = \text{Cp}$  or  $\text{Cp}^*$ ) and the nature of  $\text{X}$  (e.g.  $\text{Cl}$ ,  $\text{Br}$ ,  $\text{I}$ ,  $\text{H}$  or  $\text{Me}$ ) in this species, coupled with the spectroscopic handle afforded by the carbonyl groups, made this an attractive system. In addition, work by Beck,<sup>11,12</sup> on a series of  $[\text{Mo}]\text{-FBF}_3$  compounds  $\{[\text{Mo}] = \text{Mo}(\text{Cp})(\text{CO})_2\text{L}$ ,



$\text{L} = 2$  electron ligand) and the recent report of hydride transfer reactions in  $[\text{Mo}(\eta\text{-L})(\text{CO})_3\text{H}]$  and related compounds to afford reactive 16 electron cationic complexes of the type  $[\text{Mo}(\eta\text{-L})(\text{CO})_3]^+$ <sup>13</sup> present a firm base with which to compare and contrast the systems under investigation. Aspects of this work have been reported previously as a communication.<sup>14</sup>

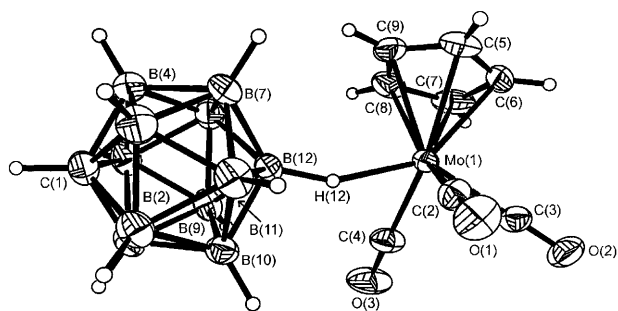


Fig. 1 Solid state structure of complex **1** showing the atom labelling scheme used. Thermal ellipsoids are shown at the 30% probability level.

## Results and discussion

Treatment of  $[\text{MoCp}(\text{CO})_3\text{Cl}]$  ( $\text{Cp} = \eta\text{-C}_5\text{H}_5$ ) with one equivalent of  $\text{Ag}[\text{CB}_{11}\text{H}_{12}]$ , **A** (see Scheme 1), in  $\text{CH}_2\text{Cl}_2$  while monitoring the CO stretching region of the IR spectrum over a period of 30 minutes initially shows the replacement of the two stretching bands associated with the starting material (2056 and  $1977\text{ cm}^{-1}$ ) with two stretching bands at higher frequency (2064 and  $1980\text{ cm}^{-1}$ ). Continued stirring for 2 days results in these latter peaks being replaced by ones at even higher wavenumber (2071 and  $2001\text{ cm}^{-1}$ ) and the concomitant formation of  $\text{AgCl}$  precipitate. This final product was identified as the zwitterionic compound  $[\text{MoCp}(\text{CO})_3(\mu\text{-H-1-CB}_{11}\text{H}_{11})]$ , **1** (see Scheme 1,  $x = 7$  or 12), formed in good yield as the only organometallic product. Compound **1** has been characterised by multinuclear NMR spectroscopy and X-ray crystallography.

The solid state structure of compound **1** is shown in Fig. 1, and salient bond lengths and angles are given in Table 1. The molecule adopts a four-legged piano-stool geometry, with the carborane anion bonded to Mo by a single 3-centre 2-electron ( $3c\text{-}2e$ ) B–H–Mo bond, affording the metal centre an overall 18 EAN count. The hydrogen atom associated with the antipodal boron atom [H(12)] was located in the difference map and freely refined. Bond lengths and angles in the cage anion are unremarkable. The cage interacts with the Mo centre *via* the antipodal B–H linkage, B(12)–H(12) [ $\text{Mo}(1) \cdots \text{B}(12)$   $3.003(3)\text{ \AA}$ ], in accordance with this being the most basic region in the cage, that is it is the vertex most susceptible to electrophilic attack.<sup>15</sup> Although the C atom was unambiguously located in the solid state structure, caution should be exercised when translating this to the solution state structure. This is demonstrated when the NMR spectroscopic data for complex **1** are taken into account (see below) which show the presence of two isomers in solution. Such potential ambiguity between solution and solid state structural assignment has previously been noted in related systems.<sup>16</sup> The antipodal cage B–H bond [H(12)] is canted off the B(12)–C(1) vector by  $18(1)^\circ$ , allowing efficient overlap between the bonding  $\sigma$  electron pair with a suitable orbital on the molybdenum centre in addition to minimising the steric interactions between the cage and the metal–ligand set. The Mo–H–B angle, at  $152(2)^\circ$ , also reflects this scenario. Other structures which have similar monodentate Mo–H–B linkages where cage hydrogen atoms have also been refined, show similar M–H–B angles, *viz.*  $[\text{Fe}(\text{Cp})(\text{CO})_2(\text{CB}_{11}\text{H}_{12})]$   $141(2)^\circ$  and  $[\text{Fe}(\text{TPP})(\text{CB}_{11}\text{H}_{12})]$  (TPP = tetraphenylphosphorynate)  $151(2)^\circ$ .<sup>6</sup>

The solution spectroscopic data for compound **1** are in broad agreement with the solid state structure. The IR spectrum shows the expected two CO stretching bands ( $A_1 + E$ ), at 2071 and  $2001\text{ cm}^{-1}$  (average  $2036\text{ cm}^{-1}$ ) shifted to higher frequency than those from  $[\text{MoCp}(\text{CO})_3\text{Cl}]$ . The bridging Mo–H(12)–B(12) atom is observed as a very broad stretch centred around  $2240\text{ cm}^{-1}$  ( $2243\text{ cm}^{-1}$  in the solid state, see Experimental section). These  $\nu_{\text{CO}}$  values can be compared with those found for  $[\text{MoCp}(\text{CO})_3(\text{FBF}_3)]$  at 2067 and  $1975\text{ cm}^{-1}$  (average  $2021\text{ cm}^{-1}$ ) and  $[\text{MoCp}(\text{CO})_3(\text{FSbF}_3)]$  at 2079 and  $2001\text{ cm}^{-1}$  (aver-

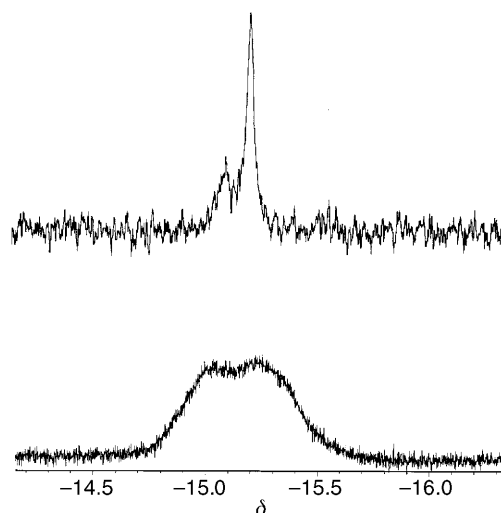


Fig. 2 High field region of the  $-90^\circ\text{C}$  (top)  $^1\text{H}\text{-}\{^{11}\text{B}\}$  and room temperature  $^1\text{H}$  (bottom) NMR spectra of compound **1** ( $\text{CD}_2\text{Cl}_2$ ).

age  $2040\text{ cm}^{-1}$ ).<sup>11</sup> Both of these latter complexes contain weakly co-ordinated anions, and on a ranking ionicity scale of the  $[\text{M}]^+ \cdots [\text{Y}]^-$  interaction using CO stretching frequencies as a guide  $\text{CB}_{11}\text{H}_{12}$  fits in between  $\text{SbF}_6$  and  $\text{BF}_4$  in this system. This order matches that found previously in  $\text{FeCp}(\text{CO})_2\text{Y}$  ( $\text{Y} = \text{non-co-ordinating anion}$ ).<sup>17</sup> The  $^1\text{H}\text{-}\{^{11}\text{B}\}$  NMR spectrum of **1** displays two peaks in the Cp region, in an approximate 1:2.5 ratio; signals are also observed due to cage C–H and B–H groups and a single, slightly broad, peak at  $\delta -15.11$  is assigned to Mo–H–B. This latter signal is observed as a partially collapsed quartet in the  $^1\text{H}$  NMR spectrum with a reduced B–H coupling constant [ $J(\text{BH})$  87 Hz], as expected for a B–H–M bond. This peak is at unusually high field relative to that expected for B–H–M linkages ( $\delta -5$  to  $-11$ ), similar to that which has been noted previously in related systems.<sup>8c</sup> On cooling to  $-90^\circ\text{C}$  the ratio of Cp resonances does not change but, due to thermal decoupling at lower temperatures, the high field resonance now is observed as two sharper peaks in the  $^1\text{H}\text{-}\{^{11}\text{B}\}$  NMR spectrum (Fig. 2) in the same ratio as the two Cp resonances. We assign these two sets of peaks to positional isomers in which the  $\text{CB}_{11}\text{H}_{12}$  cage is either bonded to the metal *via* the antipodal B(12)–H(12) bond or *via* a B–H linkage on the lower pentagonal belt. The observation of isomers in  $[\text{FeCp}(\text{CO})_2(\text{CB}_{11}\text{H}_{12})]$  and  $[\text{FeCp}(\text{CO})_2(\text{CB}_9\text{H}_{10})]$  has previously been noted by Strauss and co-workers.<sup>16</sup> For the latter, the two species are assigned as isomers in which the carborane bonds to the metal centre through an antipodal and a single lower pentagonal belt hydrogen atom respectively. Confirmation of the isomeric pair in **1** comes from inspection of the  $^{11}\text{B}\text{-}\{^1\text{H}\}$  NMR spectrum. The major peaks observed are due to a  $\text{C}_5$  symmetric carborane (assigned to the 12 isomer, assuming free rotation around the Mo–H–B vector) at  $\delta -10.4$  (1 B)  $-11.7$  (5 B) and  $-13.9$  (5 B) as well as less intense peaks, at  $\delta -4.7$  and  $-18.6$ , which we tentatively assign to the 7 isomer. The other signals for this isomer are presumably masked under the resonances for the major isomer. Coupling constants and chemical shifts are in accord with this formulation. For the 12 isomer the unique antipodal B–H appears to have a reduced coupling constant [ $J(\text{HB})$  *ca.* 90 Hz], although as this peak appears as a shoulder to a larger high field peak this value should be treated with caution. This antipodal B–H coupling may be better gleaned from the  $^1\text{H}$  NMR spectra (see above). Reduced  $J(\text{HB})$  coupling constants have ample precedent as being diagnostic of M–H–B co-ordination,<sup>18</sup> while this signal is also shifted some 6 ppm upfield from  $\text{Ag}[\text{CB}_{11}\text{H}_{12}]$ , also indicative of {B–H} co-ordination. This upfield shift on *exo* co-ordination of an anionic borane has been observed previously.<sup>19,20</sup> For the 7

isomer, the antipodal B atom resonates at  $\delta$   $-4.7$ , similar to that found for  $\text{CsCB}_{11}\text{H}_{12}$ , while a peak integrating to 1 B at  $\delta$   $-18.6$  is assigned to  $\text{B}(7)\text{--H}(7)\text{--Mo}$  which also exhibits a correspondingly smaller coupling constant [ $J(\text{HB})$  68 Hz].

Warming a sample of compound **1** in  $d_8$ -toluene to 80 °C resulted in coalescence of the two Cp peaks, demonstrating chemical exchange of the isomers, while the high field resonance at  $\delta$  *ca.*  $-15$  did not shift appreciably. Further confirmation of this exchange process comes from a  $^1\text{H}$  EXSY experiment (EXchange SpectroscopY), which shows clear exchange cross peaks between the two Cp resonances. Thus the 12 and 7 isomers in complex **1** are in slow exchange with one another in solution.

It is interesting to compare the chemical robustness of **1** with the complexes previously prepared by Beck, such as  $[\text{MoCp}(\text{CO})_3(\text{FBF}_3)]$ , which are extremely moisture sensitive and must routinely be handled at low temperature.<sup>12</sup> By contrast, **1** is stable at room temperature and can withstand handling in air for appreciable amounts of time. However, both compounds show similar frequencies for their CO stretching bands, suggesting that both  $[\text{BF}_4]^-$  and  $[\text{CB}_{11}\text{H}_{12}]^-$  possess similar weakly co-ordinating properties. This difference in chemical behaviour may arise either because the cage affords some kinetic stabilisation by virtue of its steric bulk or is intrinsically more strongly bound to the metal centre than  $[\text{BF}_4]^-$ . In support of this hypothesis, the cage anion in **1** is only replaced by strong nucleophiles such as chloride, weaker nucleophiles such as acetone or water leaving **1** unchanged after 30 minutes (according to NMR spectroscopy), while a strong  $\text{Mo--H--B}$  interaction is evidenced by the high field chemical shift and small value of  $J(\text{BH})$  associated with H(12). Although spectroscopic measurements can provide a valuable comparative guide to the weakly co-ordinating properties of this class of anion, it is apparent that, in this system at least, this may not necessarily be a unique guide to the chemical properties of the system.

Having established the identity of the final product in this metathesis reaction our attention now turned to the intermediate species observed. Although intermediates have been observed in silver salt metathesis before, notably by Mattson and Graham,<sup>21</sup> it was the work of Reed and co-workers<sup>6</sup> that first highlighted the role of the counter ion in such reactions, observing by IR spectroscopy the formation of an intermediate adduct species, postulated as  $[\text{FeCp}(\text{CO})_2\text{I}\cdot\text{AgCB}_{11}\text{H}_{12}]$ . It was suggested that the low nucleophilicity of the carborane counter ion resulted in the relatively long lifetime of this intermediate species. The corollary of this theory is that the anion is intimately involved in the rate-determining step in metathesis. However, to our knowledge, such intermediates have never been put on a firm spectroscopic or structural footing. Given the observation of an intermediate species in the reaction of  $[\text{MoCp}(\text{CO})_3\text{Cl}]$  with  $\text{Ag}[\text{CB}_{11}\text{H}_{12}]$  to afford **1**, we sought further to characterise this product. For the chloride species, IR spectroscopy revealed that the intermediate was never the sole component in solution. Moving to  $[\text{MoCp}(\text{CO})_3\text{I}]$  resulted in a slowing down of this reaction (presumably a consequence of the reduced thermodynamic driving force of  $\text{AgI}$  formation over  $\text{AgCl}$ ), so that complete metathesis took 7 days, and that after 30 minutes the only component of the reaction mixture was the intermediate species. Cessation of the reaction at this point, by cooling, followed by recrystallisation at low temperature afforded the intermediate species  $[\text{MoCp}(\text{CO})_3\text{I}\cdot\text{Ag}\{\text{CB}_{11}\text{H}_{12}\}]_2$ , **2**, in *ca.* 50% isolated yield as a red crystalline solid. Compound **2** was fully characterised by X-ray crystallography, multinuclear NMR spectroscopy, IR and micro-analysis.

The solid state structure of compound **2** is shown in Fig. 3, with relevant bond lengths and angles in Table 1. The molecule adopts a crystallographically imposed  $C_2$  dimeric structure, with each of the silver atoms bonded to an iodine from each of the  $\{\text{CpMo}(\text{CO})_3\text{I}\}$  fragments. The central core is hinged

**Table 1** Selected bond lengths (Å) and angles (°) for compounds **1** to **4**

Compound <b>1</b>			
Mo(1)–C(2)	2.011(3)	Mo(1)–C(3)	2.007(3)
Mo(1)–C(4)	2.017(3)	C(2)–O(1)	1.127(3)
C(3)–O(2)	1.123(3)	C(4)–O(3)	1.125(3)
Mo(1)–H(12)	1.90(3)	B(12)–H(12)	1.18(3)
Mo(1)⋯B(12)	3.003(3)		
Mo(1)–B(12)–C(1)	176.4(1)	Mo(1)–H(12)–B(12)	152(2)
Compound <b>2</b>			
Mo(1)–C(2)	1.997(10)	Mo(1)–C(3)	2.000(10)
Mo(1)–C(4)	2.027(9)	Mo(1)–I(1)	2.8599(8)
C(2)–O(2)	1.159(12)	O(3)–C(3)	1.22(11)
C(4)–O(4)	1.134(11)	Ag(1)–H(7)	1.96
I(1)–Ag(1)	2.9748(10)	Ag(1)–I(1A)	2.7599(9)
Ag(1)–B(7)	2.659(10)		
Ag(1A)–I(1)–Ag(1)	71.19(3)	I(1)–Ag(1)–I(1A)	97.10(3)
Compound <b>3</b>			
Mo(1)–C(2)	2.08(3)	Mo(1)–C(8)	1.99(2)
Mo(1)–C(9)	2.03(3)	C(2)–O(2)	1.09(3)
C(8)–O(1)	1.13(3)	C(9)–O(3)	1.05(3)
Mo(1)–I(1)	2.865(2)	Ag(1)–I(1')	2.980(3)
Ag(1)–I(1)	2.778(3)	Ag(1)–Br(1)	2.803(3)
Ag(1)–Br(2)	2.771(3)		
Ag(1)–I(1)–Ag(1')	81.41(8)	I(1)–Ag(1)–I(1')	98.59(8)
Br(1)–Ag(1)–Br(2)	87.24(8)	Ag(1)–I(1)–Mo(1)	107.87(7)
Ag(1')–I(1)–Mo(1)	114.20(7)		
Compound <b>4</b>			
Mo(1)–C(2)	1.988(3)	Mo(1)–C(3)	2.034(3)
Mo(1)–C(4)	2.049(3)	C(2)–O(1)	1.146(3)
C(3)–O(2)	1.128(4)	C(4)–O(3)	1.124(3)
Mo(1)–H(12)	1.97(5)	B(12)–H(12)	1.07(5)
Mo(1)–B(12)	2.969(3)		
Mo(1)–B(12)–C(1)	168.4(1)	Mo(1)–H(12)–B(12)	154(4)

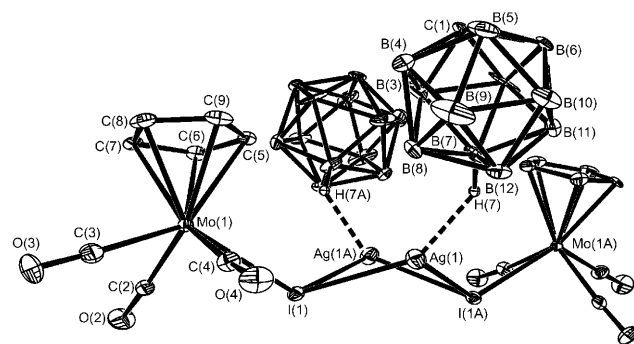


**Fig. 3** Solid state structure of complex **2**. H atoms, apart from H(7), are omitted for clarity. Equivalent atoms generated by the operation  $-x + \frac{1}{2}, -y, z$ . Other details as in Fig. 1.

around the  $\text{Mo}(1\text{A})\text{--I}(1\text{A})\text{--I}(1)\text{--Mo}(1)$  vector by 123.3°, and has significantly different Ag–I bond lengths,  $\text{Ag}(1)\text{--I}(1)$  2.9748(10) and  $\text{Ag}(1)\text{--I}(1\text{A})$  2.7599(9) Å. This difference in Ag–X distances in  $\{\text{Ag}_2\text{X}_2\}$  fragments has been observed previously,<sup>22</sup> while the Ag–I bond lengths are a little longer and shorter respectively than found in similar  $\{\text{I--Ag--I}\}$  fragments.<sup>23</sup> There are silver adduct species of transition metal halides that show similar features as to those of **2**, such as the recently reported, ion pair separated,  $[\{\text{ReTp}(\text{NC}_6\text{H}_4\text{Me-}p)(\text{Ph})\text{I}\}_2\text{Ag}][\text{PF}_6]$ <sup>24</sup> [ $\text{Tp}$  = tris-(pyrazolyl) borate] in which a single silver bridges two  $\{\text{Re--I}\}$  fragments. However, to our knowledge, **2** is the first example of a  $\{\text{Ag}_2\text{X}_2\}$  motif with appended metal fragments. The Mo–I bond distance in **2** lies within the expected range.<sup>25</sup> In the dimeric unit in **2** each silver has a close contact with a carb-

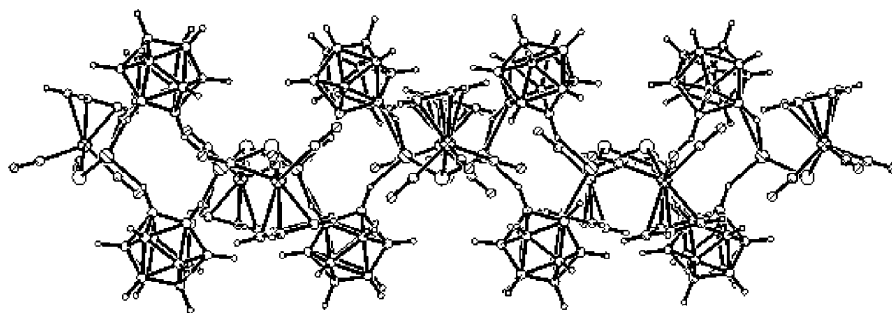


Fig. 4 The crystallographic packing diagram for complex **2** viewed along the *a* axis, showing the extended cation-anion interactions in the solid state.

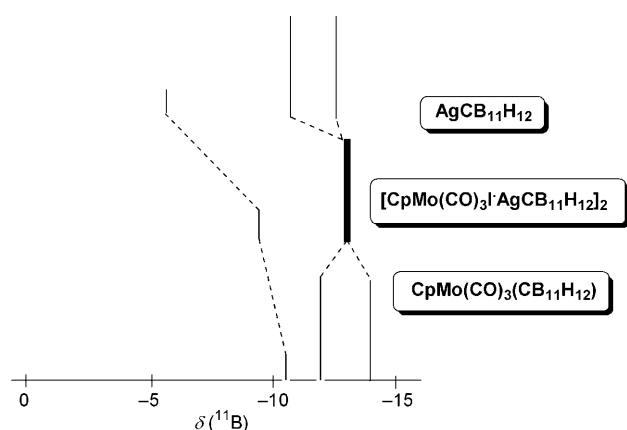


Fig. 5 Comparative  $^{11}\text{B}$  NMR 'stick' diagram of complexes **1**, **2** and  $\text{Ag}[\text{CB}_{11}\text{H}_{12}]$ .

orane anion *via* a B–H–Ag 3c–2e interaction, B(7)–H(7)–Ag(1) 1.96 Å [Ag(1)–B(7) 2.659(10) Å]. This distance is slightly longer than that observed in the recently reported complex [2,2,2-(CO)<sub>3</sub>-2-PPh<sub>3</sub>-7,12-(μ-H)<sub>2</sub>-7,12-{Ag(PPh<sub>3</sub>)}-*closo*-2,1-MoCB<sub>10</sub>-H<sub>9</sub>], in which the {Ag(PPh<sub>3</sub>)}<sup>+</sup> fragment is ligated in a dihapto manner on the surface of the cage.<sup>26</sup> The apparently vacant site around each silver atom in compound **2** is filled by an intramolecular Ag–H–B interaction. In particular, H(12) interacts with an adjacent silver [H(12)–Ag(1') 1.96 Å] to form a ribbon of alternating cation and bridging anions (Fig. 4). This bridging mode has been observed previously in the simple silver salt of [CB<sub>11</sub>H<sub>12</sub>]<sup>–</sup>, Ag[CB<sub>11</sub>H<sub>12</sub>]·2C<sub>6</sub>H<sub>6</sub>.<sup>27</sup> The Ag–H and Ag–B bond distances therein are similar to those found in complex **2**.

Although it is unlikely that the polymeric structure in complex **2** persists in solution (CH<sub>2</sub>Cl<sub>2</sub>), evidence for interaction between the cage and silver comes from inspection of the NMR spectroscopic data. The  $^1\text{H}$ – $^{11}\text{B}$  NMR spectrum shows only one Cp resonance, at  $\delta$  5.75, with the expected peaks due to C–H and B–H groups observed in the range  $\delta$  2.56 to 1.86. No high field resonances were observed, even on cooling of the sample to –80 °C. The room temperature  $^{11}\text{B}$  NMR spectrum shows two peaks at  $\delta$  –9.11 and –12.65 in the ratio 1 : 10 (the latter peak representing a 5 + 5 coincidence), indicating C<sub>3</sub> symmetry in solution, and thus rapid site exchange of Ag–H–B interactions. These resonances are significantly shifted relative to those of 'free' Ag[CB<sub>11</sub>H<sub>12</sub>]. This change is better seen in a stick diagram (Fig. 5), which shows the relationship between the  $^{11}\text{B}$  resonances of **1**, **2** and Ag[CB<sub>11</sub>H<sub>12</sub>]. The boron atoms that are involved in bonding to the metal centre (either Ag or Mo) are shifted upfield. Thus in **1** (only the 12 isomer is shown) only the unique boron atom resonance is shifted appreciably. Evidence for B–H interactions in **2** is demonstrated by both the upfield shift of B(12) from that found for Ag[CB<sub>11</sub>H<sub>12</sub>] ( $\Delta\delta_{11\text{B}}$  *ca.* 4 ppm) and the boron atoms associated with the lower pentagonal belt ( $\Delta\delta_{11\text{B}}$  *ca.* 2 ppm). In agreement with this observation, the B–H coupling constant in **2** for the unique boron

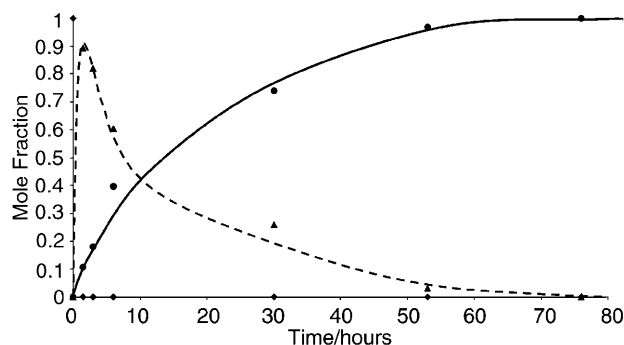


Fig. 6 Graph of the relative concentration of species **1**, **2** and [MoCp(CO)<sub>3</sub>I] against time in CD<sub>2</sub>Cl<sub>2</sub> at room temperature. ▲ [MoCp(CO)<sub>3</sub>I]·Ag(CB<sub>11</sub>H<sub>12</sub>)<sub>2</sub>, ◆ [MoCp(CO)<sub>3</sub>I] and ● [MoCp(CO)<sub>3</sub>(CB<sub>11</sub>H<sub>12</sub>)]; relative concentrations measured as the integral values of the respective Cp resonances of each complex.

atom is slightly smaller than that found in Ag[CB<sub>11</sub>H<sub>12</sub>] (119 vs. 125 Hz respectively). These chemical shifts suggest that in solution both the antipodal and lower pentagonal belt B–H groups interact with Ag, similar to the η<sup>2</sup>-bidentate co-ordination found in [Rh(COD)(CB<sub>11</sub>H<sub>12</sub>)] in which the {Rh(COD)}<sup>+</sup> fragment is fluxional over the surface of the cage.<sup>28</sup> Further evidence for this unusual central core in solution comes from the  $^{109}\text{Ag}$  resonance for **2**,  $\delta$  1335, which is significantly shifted from that normally found for silver(I)<sup>29</sup> complexes [*ca.*  $\delta$  500].

In order conclusively to prove that complex **2** is an intermediate on the pathway to **1** the reaction between [MoCp(CO)<sub>3</sub>I] and Ag[CB<sub>11</sub>H<sub>12</sub>] in CD<sub>2</sub>Cl<sub>2</sub> was monitored by  $^1\text{H}$  NMR spectroscopy. The time dependent concentration profile of this reaction is shown in Fig. 6. This clearly shows the rapid formation of **2** and its gradual disappearance with concomitant growth of complex **1**. The mass balance of the system remains constant showing that **2** converts smoothly into **1**.

Having prepared complex **1**, *via* the intermediate species **2**, we were interested in investigating the silver salt metathesis reaction of [MoCp(CO)<sub>3</sub>X] with the even more non-nucleophilic, more weakly co-ordinating anion [CB<sub>11</sub>Br<sub>6</sub>H<sub>6</sub>]<sup>–</sup>, **B**. Reaction of [MoCp(CO)<sub>3</sub>Cl] with Ag[CB<sub>11</sub>H<sub>12</sub>] did not result in any observable reaction by IR, only unchanged starting materials returned after 7 days stirring at room temperature. The parallel reaction using [MoCp(CO)<sub>3</sub>I], with the softer iodide atom, resulted in a gradual shift to higher wavenumber of the CO stretching bands over *ca.* 1 hour, moving to 2055 and 1975 cm<sup>–1</sup> which are very similar, but slightly higher, than those found for **2**.  $^1\text{H}$ ,  $^{11}\text{B}$  NMR spectroscopy and X-ray crystallography characterised this new species as [MoCp(CO)<sub>3</sub>I·Ag(CB<sub>11</sub>Br<sub>6</sub>H<sub>6</sub>)<sub>2</sub>], **3**.

The solid state structure of complex **3**, shown in Fig. 7, bears close similarities with that found in **2**, with a centrosymmetric central {Ag<sub>2</sub>I<sub>2</sub>} core appended with two {CpMo(CO)<sub>3</sub>} fragments and two bidentate CB<sub>11</sub>Br<sub>6</sub>H<sub>6</sub> cages. The two metal fragments are orientated *trans* with respect to one another and

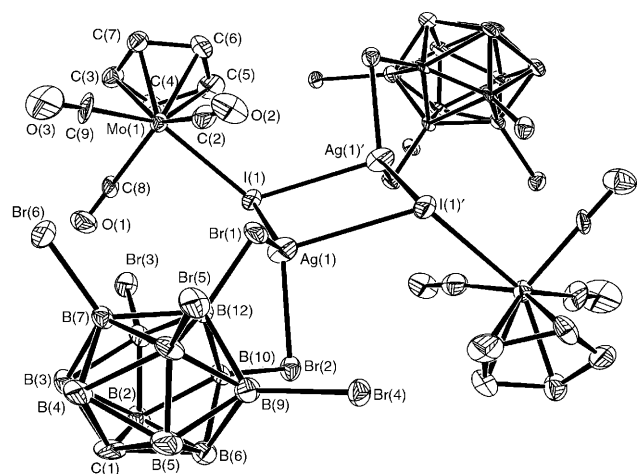


**Fig. 7** Solid state structure of complex **3**. H atoms are omitted for clarity. Equivalent atoms generated by the operation  $-x, -y, -z$ . Other details as in Fig. 1.

the central  $\{Ag_2I_2\}$  core. This central core in **3** is planar, unlike that in **2**. In fact the  $\{Ag_2I_2\}$  rhomboid is similar to that found in  $[Ag_2X_2(PPh_3)_4]^{22}$  ( $X = Cl$  or  $Br$ ) which also contains four-coordinate silver. The hexabromocarbaborane co-ordinates to the silver atoms in a bidentate manner reminiscent of that found in the simple silver salts  $Ag[CB_{11}H_6Cl_6] \cdot C_6H_6$ ,<sup>30</sup>  $Ag[1-CH_3-CB_{11}Br_{10}H] \cdot C_6H_4Me_2 \cdot p$ .<sup>31</sup> The Ag–Br bonds lengths in **3** [Ag(1)–Br(1) 2.803(3), Ag(1)–Br(2) 2.771(3) Å] are slightly shorter than generally found for both  $Ag[CB_{11}Br_6H_6]$  and related complexes<sup>31,32</sup> and dibromoalkane complexes of silver.<sup>10</sup>

The  $^1H$  NMR spectrum of complex **3** shows two Cp resonances, in the approximate ratio 1 : 8, at  $\delta$  5.84 and 5.73 respectively, with a broad peak having a high field shoulder centred at  $\delta$  2.79 assigned to the cage C–H resonances. The  $^{109}Ag$  NMR spectrum also shows two peaks, in the same approximate ratio as found in the  $^1H$  NMR spectrum, at  $\delta$  1335 (relative intensity 8) and 1325 (1). We assign these pairs of peaks to two isomers in solution, one in which the Cp groups are *trans* and the other in which the Cp groups are *cis* to one another, with respect to the central  $\{Ag_2I_2\}$  core. Both of these isomers retain equivalent Cp groups in solution (local  $C_2$  and  $C_{2v}$  symmetry respectively), assuming facile libration around the Mo(1)–I(1) bond, consistent with the NMR data. The  $^{11}B$  NMR spectrum displays three resonances in the ratio 1 : 5 : 5, suggesting either dissociation of the carbaborane in solution or rapid site exchange of Ag–Br–B interactions. Support of the latter comes from the observation of very similar  $^{109}Ag$  NMR chemical shifts for **3** and **2** implying similar structures in solution. Dissolution of crystalline **3** generates an identical spectrum, with the same ratio of isomers observed.

Complex **3** remains unchanged when in  $CH_2Cl_2$  solution for 7 days, with no metathesis product or decomposition observed (by  $^1H$  NMR and IR spectroscopy). This is consonant with the low nucleophilicity of  $[CB_{11}Br_6H_6]^-$  and the involvement of the anion in the rate-determining step in silver halide metathesis, by effectively halting metathesis at the intermediate stage in **3**. Addition of two equivalents of  $Ag[CB_{11}H_{12}]$  to a  $CH_2Cl_2$  solution of **3** results in immediate change in the IR spectrum to afford **2** which then gradually (7 days) changes to yield **1** in essentially quantitative yield. This result suggests that kinetic factors (*i.e.* the relative nucleophilicities of the anions) control the outcome of reaction in this system. Although there has been a recent brief report of arrested silver salt metathesis in  $R_3SiI$  systems,<sup>1</sup> to our knowledge this is the first fully characterised example involving a transition metal halide species in such a reaction that is clearly dependent only on the anion.

Reaction of  $Ag[CB_{11}H_{12}]$  with the sterically more demanding  $[MoCp^*(CO)_3Cl]$  [ $Cp^* = \eta^5-C_5Me_5$ ] in  $CH_2Cl_2$  resulted in a move to higher wavenumbers of the carbonyl stretches in

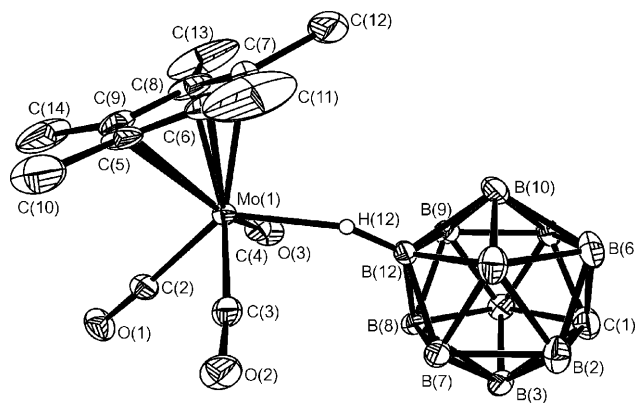


**Fig. 8** Solid state structure of complex **4**. H atoms, apart from H(12), are omitted for clarity. Other details as in Fig. 1.

the IR spectrum, but the  $^1H$  NMR spectrum showed at least 5 Cp\* peaks for the reaction mixture. Failing to cleanly abstract halide from  $[MoCp^*(CO)_3Cl]$ , an alternative method of introducing the carbaborane anion in to the co-ordination sphere was needed. Spencer and co-workers have demonstrated that reaction of  $[H(OEt_2)_2][CB_{11}H_{12}]$  with  $[PtR_2(L-L)]$  ( $R = Me$  or  $CH_2Bu^t$ ,  $L-L =$  bidentate phosphine) affords complexes in which the carbaborane is  $\eta^2$  ligated through two B–H–Pt bonds, *via* elimination of two equivalents of the corresponding alkane.<sup>7</sup> In this spirit, reaction of  $[H(OEt_2)_2][CB_{11}H_{12}]$  with  $[MoCp^*(CO)_3Me]$  at  $-78^\circ C$  afforded, on warming to room temperature, the new complex  $[MoCp^*(CO)_3(x-\mu-H-1-CB_{11}H_{11})]$  **4** ( $x = 7$  or  $12$ ) in essentially quantitative yield. The IR spectrum of this solution shows two CO stretching bands at 2057 and 1986  $cm^{-1}$ , with a broad weak peak at 2229  $cm^{-1}$  assigned to the Mo–H–B stretch. The isolation of **4** indicates that the failure of the silver salt metathesis is not due to steric hindrance in the final complex, and is perhaps due to steric interactions in a condensed intermediate species similar to **2**. The solid state structure of **4** is shown in Fig. 8, and selected bond lengths and angles are given in Table 1. The carbaborane anion in complex **4** is bound *via* the antipodal boron atom in the expected B–H–M 3c–2e bond, with the bridging hydrogen atom located and freely refined. Given the increased bulk of the Cp\* ligand it is perhaps somewhat surprising that the Mo(1)–B(12) distance [2.969(3) Å] is slightly shorter than in **1**. The only gross structural difference between **1** and **4** is that the carbaborane ligand in the latter is tilted further away from the Cp\* ring, in contrast to **1** where the carbaborane anion is closer to the Cp ring. This does not significantly effect the Mo–H(12)–B(12) angle which at  $154(4)^\circ$  is broadly similar.

The  $^1H$  and  $^{11}B$  NMR spectra demonstrate the presence of an isomeric pair in solution, as found for complex **1**, which is assigned to  $[Mo(Cp^*)(CO)_3(x-\mu-H-1-CB_{11}H_{11})]$  ( $x = 12$  or  $7$ ). Thus, two Cp\* peaks are observed at  $\delta$  2.08 and 2.04 in the ratio 1 : 3, a situation that is mirrored in the  $^{11}B$  NMR spectrum with two sets of peaks also seen. As found for **1** it is the 12 isomer that is the major component in solution. Although the structural metrics in **4** are similar to those in **1**, the increased steric bulk in **4** is manifested by the lower coalescence temperature for the fast exchange limit of the two isomers. Heating the sample to  $40^\circ C$  (compared with  $80^\circ C$  for **1**) afforded a single sharp line in the Cp\* region of the  $^1H$  NMR spectrum. The bridging hydrogen is observed in complex **4** as a partially collapsed quartet, centred at  $\delta$  –13.5, slightly to lower field than that found for **1** indicating a weaker (*i.e.* less hydridic) Mo–H–B bond. This signal also has a larger coupling constant [ $J(HB)$  98 Hz], as expected for a weaker Mo–H–B interaction. Reflecting this less intimate Mo–H–B bond compared with that in **1**, addition of water rapidly (<5 minutes) displaces the cage anion from the co-ordination sphere of the metal fragment.

**Table 2** Crystallographic data for the new complexes **1** to **4**

	1	2	3	4
Empirical formula	C <sub>9</sub> H <sub>17</sub> B <sub>11</sub> MoO <sub>3</sub>	C <sub>9</sub> H <sub>17</sub> AgB <sub>11</sub> IMoO <sub>3</sub>	C <sub>9</sub> H <sub>11</sub> AgB <sub>11</sub> Br <sub>6</sub> IMoO <sub>3</sub>	C <sub>14</sub> H <sub>27</sub> B <sub>11</sub> MoO <sub>3</sub>
Formula weight	388.08	622.85	1096.26	458.21
<i>T</i> /K	293(2)	120(2)	170(2)	170(2) K
Crystal system	Monoclinic	Orthorhombic	Triclinic	Orthorhombic
Space group	<i>P</i> 2 <sub>1</sub> / <i>c</i>	<i>Pnma</i>	<i>P</i> $\bar{1}$ (no. 2)	<i>P</i> 2 <sub>1</sub> 2 <sub>1</sub>
<i>a</i> /Å	10.1425(19)	13.8843(4)	7.7200(7)	9.75770(10)
<i>b</i> /Å	10.4875(13)	15.7193(4)	11.8360(8)	14.1357(2)
<i>c</i> /Å	16.515(2)	18.1490(6)	14.7530(15)	16.2310(2)
<i>a</i> /°			90.871(5)	
<i>β</i> /°	93.76		96.678(4)	
<i>γ</i> /°			90.355(5)	
<i>U</i> /Å <sup>3</sup>	1752.9(4)	3961.0(2)	1338.7(2)	2238.77(5)
<i>Z</i>	4	8	2	4
<i>μ</i> /mm <sup>−1</sup>	0.749	3.186	11.320	0.598
Reflections collected	4157	7282	11052	25921
Independent reflections	3801 [ <i>R</i> <sub>int</sub> = 0.0150]	3870 [ <i>R</i> <sub>int</sub> = 0.0476]	4679 [ <i>R</i> <sub>int</sub> = 0.0967]	5110 [ <i>R</i> <sub>int</sub> = 0.0276]
Final <i>R</i> <sub>1</sub> , <i>wR</i> <sub>2</sub> indices [ <i>I</i> > 2σ( <i>I</i> )]	0.0289, 0.0780	0.0563, 0.1101	0.0917, 0.2541	0.0295, 0.0859
(all data)	0.0369, 0.0806	0.0725, 0.1145	0.1324, 0.2844	0.0302, 0.0870

## Experimental

### General

All manipulations were carried out under an argon atmosphere using standard Schlenk line or dry-box techniques. CH<sub>2</sub>Cl<sub>2</sub> was distilled from CaH<sub>2</sub>, hexane from sodium.<sup>33</sup> NMR spectra were measured on a Varian-400 or JEOL-270 FT-NMR spectrometer in CD<sub>2</sub>Cl<sub>2</sub> solutions. Residual protio solvent was used as reference (CD<sub>2</sub>Cl<sub>2</sub>, δ 5.33) in <sup>1</sup>H NMR, BF<sub>3</sub>·OEt<sub>2</sub> (external) in <sup>11</sup>B NMR spectra. Infrared spectra were measured on a Perkin-Elmer 1600 FT spectrometer. Elemental analysis was performed in-house in the Department of Chemistry, University of Bath. The complexes [MoCp(CO)<sub>3</sub>X] (X = Cl or I),<sup>34</sup> [MoCp\*(CO)<sub>3</sub>Me],<sup>35</sup> Ag[CB<sub>11</sub>H<sub>12</sub>],<sup>27</sup> Ag[CB<sub>11</sub>Br<sub>6</sub>H<sub>6</sub>]<sup>6</sup> and [H(OEt<sub>2</sub>)<sub>x</sub>][CB<sub>11</sub>H<sub>12</sub>]<sup>36</sup> were prepared by the published literature routes or variations thereof.

### Preparations

**[MoCp(CO)<sub>3</sub>(CB<sub>11</sub>H<sub>12</sub>)] 1.** From [MoCp(CO)<sub>3</sub>Cl]. The compounds [MoCp(CO)<sub>3</sub>Cl] (0.134 g, 0.48 mmol) and Ag[CB<sub>11</sub>H<sub>12</sub>] (0.120 g, 0.48 mmol) were stirred in 30 ml of CH<sub>2</sub>Cl<sub>2</sub> in the dark for 2 days. The solution was filtered through Celite and solvent removed *in vacuo* to leave 0.158 g (0.41 mmol, 85% yield) of a red-brown solid. Crystals suitable for an X-ray diffraction study were grown by dissolving the solid up in the minimum of CH<sub>2</sub>Cl<sub>2</sub>, layering with hexane and then placing in a freezer overnight at −30 °C to yield 0.82 g (0.21 mmol) of dark red crystals: yield 44%. δ<sub>H</sub>(400 MHz, CD<sub>2</sub>Cl<sub>2</sub>, 22 °C) 5.86\*, 5.79 (5H, s), 2.53 (1H, s), 1.79 (5H, s), 1.66 (5H, s) and −15.11 [1H, partially collapsed quartet, *J*(BH) 87 Hz]. δ<sub>11B</sub>(128 MHz, CD<sub>2</sub>Cl<sub>2</sub>) −4.72\* [1B, d, *J*(HB) *ca.* 151], −10.41 [1B, d, sh, *J*(HB) *ca.* 90], −11.72 [5B, d, *J*(HB) 151], −13.85 [5B, d, *J*(HB) 151] and −18.56\* [1B, d, *J*(HB) 68 Hz]. Values with an asterisk indicate peaks of the 7 isomer. Found: C, 27.9; H, 4.4%. Calc. for C<sub>9</sub>H<sub>17</sub>B<sub>11</sub>MoO<sub>3</sub>: C, 27.9; H, 4.4%. IR (cm<sup>−1</sup>): (KBr) 2582m, 2549m, 2243w (broad), 2067s, 1991s and 1980s; (CH<sub>2</sub>Cl<sub>2</sub>) 2573m, 2230w, br, 2071s and 2001s, br.

From [MoCp(CO)<sub>3</sub>I]. The compounds [MoCp(CO)<sub>3</sub>I] (0.029 g, 0.080 mmol) and Ag[CB<sub>11</sub>H<sub>12</sub>] (0.021 g, 0.84 mmol) were stirred in 20 ml of CH<sub>2</sub>Cl<sub>2</sub> in the dark for 7 days. Work up was identical to that above and 0.025 g (0.064 mmol) of a red-brown solid was obtained in 81% yield. IR and NMR spectroscopic data identical to those from the previous method.

**[MoCp(CO)<sub>3</sub>I·Ag(CB<sub>11</sub>H<sub>12</sub>)]<sub>2</sub> 2.** The compounds [MoCp(CO)<sub>3</sub>I] (0.044 g, 0.12 mmol) and Ag[CB<sub>11</sub>H<sub>12</sub>] (0.030 g, 0.12 mmol) were stirred in 30 ml of CH<sub>2</sub>Cl<sub>2</sub> in the dark. After 3.5

hours the solution was filtered through Celite and solvent removed *in vacuo* in the dark, to leave 0.037 g (0.095 mmol, 79% yield) of a light sensitive red solid. Crystals suitable for an X-ray diffraction study were grown by dissolving the solid in the minimum of CH<sub>2</sub>Cl<sub>2</sub>, layering with hexane, and placing in a freezer overnight at −30 °C. δ<sub>H</sub>(400 MHz, CD<sub>2</sub>Cl<sub>2</sub>) 5.75 (5H, s), 2.56 (1H, s, C<sub>cage</sub>H), 2.12 (1H, s, BH) and 1.86 (10H, 5+5 coincidence, s, BH). δ<sub>11B</sub>(128 MHz, CD<sub>2</sub>Cl<sub>2</sub>) −9.11 [1B, d, *J*(BH) 119] and −12.65 [10B, d, 5+5 coincidence, *J*(BH) 144 Hz]. δ<sub>109Ag</sub>(19MHz, CD<sub>2</sub>Cl<sub>2</sub>) 1335 (s). Found: C, 17.8; H, 2.8. Calc. for C<sub>9</sub>H<sub>17</sub>AgB<sub>11</sub>IMoO<sub>3</sub>: C, 17.4; H, 2.7%. IR (cm<sup>−1</sup>): (KBr) 2556m, 2531m, 2041s, 1971s and 1950s; (CH<sub>2</sub>Cl<sub>2</sub>) 2570m, 2054s and 1973s br.

**[MoCp(CO)<sub>3</sub>I·Ag(CB<sub>11</sub>Br<sub>6</sub>H<sub>6</sub>)]<sub>2</sub> 3.** Ag[CB<sub>11</sub>Br<sub>6</sub>H<sub>6</sub>] (0.060 g, 0.083 mmol) and [MoCp(CO)<sub>3</sub>I] (0.028 g, 0.075 mmol) were stirred in 20 ml of CH<sub>2</sub>Cl<sub>2</sub> in the dark for 5 hours. The red solution formed was filtered through Celite and the solvent removed from the filtrate *in vacuo* to leave a red solid. Crystals suitable for an X-ray diffraction study were grown by redissolving the solid product in the minimum of CH<sub>2</sub>Cl<sub>2</sub> and allowing slow evaporation of solvent under a flow of argon to yield 0.041 g (0.021 mmol, yield 56%) of dark red crystals. δ<sub>H</sub>(400 MHz, CD<sub>2</sub>Cl<sub>2</sub>) 5.84 (s, peak from isomer), 5.73 (5H, s) and 2.79 (1H, s). δ<sub>11B</sub>(128 MHz, CD<sub>2</sub>Cl<sub>2</sub>) −0.7 (1B, s), −7.86 (5B, s) and −17.94 [d, 5B, *J*(BH) 152 Hz]. δ<sub>109Ag</sub>(19 MHz, CD<sub>2</sub>Cl<sub>2</sub>) 1335 (s, relative intensity 8) and 1325 (s, 1). Found: C, 9.18; H, 1.11. Calc. for C<sub>9</sub>H<sub>11</sub>AgB<sub>11</sub>Br<sub>6</sub>IMoO<sub>3</sub>: C, 9.86; H, 1.00%. IR (CH<sub>2</sub>Cl<sub>2</sub>, cm<sup>−1</sup>): 2613w, 2055s and 1975s br.

**[MoCp\*(CO)<sub>3</sub>(CB<sub>11</sub>H<sub>12</sub>)] 4.** The compound [H(OEt<sub>2</sub>)<sub>x</sub>][CB<sub>11</sub>H<sub>12</sub>] (0.007 g, 0.039 mmol (assuming *x* = 2)) was measured into a pre-weighed Schlenk vessel at −78 °C. To this was added a solution of [MoCp\*(CO)<sub>3</sub>Me] (0.014 g, 0.042 mmol) in 20 ml of CH<sub>2</sub>Cl<sub>2</sub> with stirring at −78 °C. A change from yellow to orange-red was observed as the reactant mixture was allowed to warm slowly to room temperature. The IR spectrum indicated the reaction had only reached approximately 30% completion. A second 10 mg portion of [H(OEt<sub>2</sub>)<sub>x</sub>][CB<sub>11</sub>H<sub>12</sub>] was added and another IR spectrum taken 5 minutes later indicated all of the [MoCp\*(CO)<sub>3</sub>Me] starting material had been consumed. The solvent was removed *in vacuo* and the <sup>1</sup>H NMR spectrum of the red solid formed indicated no starting material or excess of [H(OEt<sub>2</sub>)<sub>x</sub>][CB<sub>11</sub>H<sub>12</sub>] present. A <sup>11</sup>B NMR spectrum of the contents of the cold trap of the Schlenk line showed the presence of [H(OEt<sub>2</sub>)<sub>x</sub>][CB<sub>11</sub>H<sub>12</sub>]. The product was re-dissolved in the minimum of CH<sub>2</sub>Cl<sub>2</sub>, layered with hexane and stored in a freezer at −30 °C to afford orange-red crystals suitable for an X-ray diffraction study. δ<sub>11B</sub>(400 MHz, CD<sub>2</sub>Cl<sub>2</sub>) 2.51 (1H, s, br),

2.08\*, 2.04 (15H, s) and -13.5 [1H, partially collapsed quartet,  $J(\text{BH})$  98 Hz].  $\delta_{11\text{B}}$  (128 MHz,  $\text{CD}_2\text{Cl}_2$ ) -5.15 [1B, d,  $J(\text{HB})$  128]\*, -10.62 [1B, d, sh], -11.91 [5B, d,  $J(\text{HB})$  150], -13.94 [5B, d,  $J(\text{HB})$  167] and -18.79 [1 B, d br,  $J(\text{HB})$  ca. 65 Hz]\* (values with an asterisk indicate peaks relating to the 7 isomer of the product). IR ( $\text{CH}_2\text{Cl}_2$ ,  $\text{cm}^{-1}$ ): 2571m, 2229w br, 2057s and 1986s br.

### X-Ray crystallography

The crystal structure data for compound **1** were collected on an Enraf-Nonius CAD4 diffractometer, those for **2**, **3** and **4** on a Nonius KappaCCD. Structure solution followed by full-matrix least squares refinement was performed using the SHELX suite of programs throughout.<sup>37</sup> Hydrogens were included at calculated positions in all cases except for H12 in **1** and **4**. In these instances the hydrogen atom was readily located in the penultimate difference Fourier electron density map and allowed to refine freely. The crystal data presented for **3** arose from the fourth data set collected on a crystal from the batch, in an effort to improve the quality of the refinement. Although the mosaicity of the final crystal selected ( $0.874^\circ$ ) was not excessive, it does not adequately reflect the poor peak profiles observed during data frames. However, the data quality is reflected in the errors on the unit cell parameters, the  $R$  values and in the large peak and hole that are manifest in the final difference Fourier map despite the small sample size and application of an absorption correction. A brief perusal of the thermal displacement parameters of complex **4** suggests that there might be some libration in the pentamethylcyclopentadienyl ring. Unfortunately, stringent efforts to model this disorder failed consistently. Crystal data are summarised in Table 2.

CCDC reference number 186/2282.

See <http://www.rsc.org/suppdata/du/b0/b008222h/> for crystallographic files in .cif format.

### Acknowledgements

The Royal Society (A. S. W.) and the University of Bath (N. J. P.) are thanked for financial support. The JREI/EPSC and The University of Bath are thanked for providing funds to purchase an X-ray diffractometer at Bath. The EPSRC and King's College London are thanked for provision of the X-ray diffractometer and the Nuffield Foundation for computing equipment (J. W. S.). Dr Jonathon Rourke is thanked for his assistance in obtaining the  $^{109}\text{Ag}$  NMR spectra, Dr Georgina M. Rosair is thanked for initial structural investigations on complex **1**.

### References

- C. A. Reed, *Acc. Chem. Res.*, 1998, **31**, 133.
- S. H. Strauss, *Chem. Rev.*, 1993, **93**, 927.
- C. A. Reed, N. L. P. Fackler, K.-C. Kim, D. Stasko, D. R. Evans, P. D. W. Boyd and C. E. F. Rickard, *J. Am. Chem. Soc.*, 1999, **121**, 6314.
- A. J. Lupinetti, M. D. Havighurst, S. M. Miller, O. R. Anderson and S. H. Strauss, *J. Am. Chem. Soc.*, 1999, **121**, 1190.
- D. J. Crowther, S. L. Borkowsky, D. Swenson, T. Y. Meyer and R. F. Jordan, *Organometallics*, 1993, **12**, 2897.
- D. J. Liston, Y. J. Lee, W. R. Scheidt and C. A. Reed, *J. Am. Chem. Soc.*, 1989, **111**, 6643; K. Shelly, C. A. Reed, Y. J. Lee and W. R. Scheidt, *J. Am. Chem. Soc.*, 1986, **108**, 3117.
- G. S. Mhinzi, S. A. Litster, A. D. Redhouse and J. L. Spencer, *J. Chem. Soc., Dalton Trans.*, 1991, 2769.
- (a) D. D. Ellis, A. Franken, P. A. Jelliss, J. A. Kautz, F. G. A. Stone and P.-Y. Yu, *J. Chem. Soc., Dalton Trans.*, 2000, 2509; (b) J. C. Jeffery, P. A. Jelliss, L. H. Rees and F. G. A. Stone, *Organometallics*, 1998, **17**, 2258; (c) D. D. Ellis, P. A. Jelliss and F. G. A. Stone, *Organometallics*, 1999, **18**, 4982.
- E. Y.-X. Chen and T. J. Marks, *Chem. Rev.*, 2000, **100**, 1391.
- D. M. Van Seggen, P. K. Hurlburt, O. P. Anderson and S. H. Strauss, *Inorg. Chem.*, 1995, **34**, 3453.
- W. Beck and K. Sünkel, *Chem. Rev.*, 1988, **88**, 1405.
- W. Beck, *Inorg. Synth.*, 1990, **28**, 1.
- T.-Y. Cheng, B. S. Brunshwig and R. M. Bullock, *J. Am. Chem. Soc.*, 1998, **120**, 13121.
- N. J. Patmore, J. W. Steed and A. S. Weller, *Chem. Commun.*, 2000, 1055.
- T. Jelinek, P. Baldwin, W. R. Scheidt and C. A. Reed, *Inorg. Chem.*, 1993, **32**, 1982.
- S. V. Ivanov, J. J. Rockwell, S. M. Miller, O. P. Anderson, K. A. Solntsev and S. H. Strauss, *Inorg. Chem.*, 1996, **35**, 7882.
- Z. Xie, T. Jelinek, R. Bau and C. A. Reed, *J. Am. Chem. Soc.*, 1994, **116**, 1907.
- S. A. Brew and F. G. A. Stone, *Adv. Organomet. Chem.*, 1993, **35**, 135.
- M. Elrington, N. N. Greenwood, J. D. Kennedy and M. Thornton-Pett, *J. Chem. Soc., Dalton Trans.*, 1987, 451.
- Interestingly, *metallo-carboranes* with *exo* co-ordinated metal fragments and a metal-metal bond show downfield shifts of the involved boron atoms,<sup>18</sup> opposite to that found for  $\text{CB}_{11}\text{H}_{12}$  and other *closo* carboranes and boranes, while the addition of bridging hydrogen atoms across M-B bonds in  $\text{M}_y\text{B}_x$  species normally shifts  $^{11}\text{B}$  resonances upfield (N. P. Rath and T. P. Fehlner, *J. Am. Chem. Soc.*, 1987, **109**, 5273).
- B. M. Mattson and W. A. G. Graham, *Inorg. Chem.*, 1981, **20**, 3186.
- G. A. Bowmaker, Effendy, J. V. Hanna, P. C. Healy, B. W. Skelton and A. H. White, *J. Chem. Soc., Dalton Trans.*, 1993, 1387.
- T. N. Sal'nikova, V. G. Andrianov and Yu. T. Struchkov, *Koord. Khim.*, 1976, 707.
- W. S. McNeil, D. D. DuMez, Y. Matano, S. Lovell and J. M. Mayer, *Organometallics*, 1999, **18**, 3715.
- See for example M. A. Bush, A. D. U. Hardy, L. Manojlovic-Muir and G. A. Sim, *J. Chem. Soc. A*, 1971, 1003.
- D. D. Ellis, A. Franken, P. A. Jelliss, J. A. Kautz, F. G. A. Stone and P.-Y. Yu, *J. Chem. Soc., Dalton Trans.*, 2000, 2509.
- K. Shelly, D. C. Finster, Y. J. Lee, W. R. Scheidt and C. A. Reed, *J. Am. Chem. Soc.*, 1985, **107**, 5955.
- A. S. Weller, M. F. Mahon and J. W. Steed, *J. Organomet. Chem.*, 2001, **614-615**, 113.
- R. Eujen, B. Hoge and D. J. Brauer, *Inorg. Chem.*, 1997, **36**, 1464.
- Z. Xie, B.-M. Wu, T. C. W. Mak, J. Manning and C. A. Reed, *J. Chem. Soc., Dalton Trans.*, 1997, 1213.
- Z. Xie, C.-W. Tsang, E. T.-P. Sze, Q. Yang, D. T. W. Chan and T. C. W. Mak, *Inorg. Chem.*, 1998, **37**, 6444.
- Z. Xie, R. Bau and C. A. Reed, *Angew. Chem., Int. Ed. Engl.*, 1994, **33**, 2433.
- D. F. Shriver and M. A. Drezdon, *The Manipulation of Air-Sensitive Compounds*, 2nd edn., Wiley-Interscience, New York, 1986.
- T. S. Piper and G. Wilkinson, *J. Inorg. Nucl. Chem.*, 1956, **3**, 104.
- R. B. King and M. B. Bisnette, *J. Organomet. Chem.*, 1967, **8**, 287.
- T. Jelinek, J. Plešek, S. Hermanek and B. Stibr, *Collect. Czech. Chem. Commun.*, 1986, **51**, 819.
- G. M. Sheldrick, SHELX 97, A computer program for refinement of crystal structures, University of Göttingen, 1997.